20

Immersion skin clearing using an aqueous urea solution: optical coherence tomography data and molecular modeling

© K.V. Berezin[1], E.Yu. Stepanovich[2], A.M. Likhter[2], K.N. Dvoretsky[3], E.V. Grabarchuk[2], I.Yu. Yanina[1,4], V.V. Tuchin[1,4,5]

[1] Saratov National Research State University, Saratov, Russia
[2] Astrakhan State University, Astrakhan, Russia
[3] Saratov State Medical University, Saratov, Russia
[4] Tomsk State University, Tomsk, Russia
[5] Institute of Precision Mechanics and Control Problems, FRC „Saratov Scientific Centre of the Russian Academy of Sciences", Saratov, Russia

e-mail: berezinkv@yandex.ru

Received June 05, 2025
Revised August 08, 2025
Accepted November 25, 2025

Using optical coherence tomography, we obtained results from immersion optical clearing of human skin *in vivo* using a 50 % aqueous urea solution as the immersion agent. To assess the effectiveness of optical clearing, we determined the rate of change of the light scattering coefficient using an averaged A-scan of the optical coherence tomography signal in a dermal region at a depth of 350 to 700 μm. Molecular modeling using full-atom molecular dynamics (GROMACS) methods determined the effect of a 50 % aqueous urea solution on the spatial volume of a collagen microfibril fragment. $5((GPH)_{12})_3$ Using HF/STO3G/DFT/B3LYP/6-311G(d) quantum chemistry methods, the intermolecular interaction energy in a urea complex with a collagen peptide fragment $((GPH)_3)_2$ was calculated. The parameters of the regression equation relating the optical clearing efficiency to the intermolecular interaction energy were refined. The thermodynamics of the hydrogen bonds formed during the interaction of urea with the collagen peptide and water molecules was discussed.

Keywords: Molecular modeling, optical clearing of human skin, hydrogen bond thermodynamics, molecular dynamics, quantum chemistry, urea.

DOI: 10.61011/EOS.2025.12.63179.37-25

Introduction

The use of modern photomedicine and biomedical optics technologies in the diagnosis and treatment of diseases faces limitations associated with pronounced light scattering in the skin and most biological tissues in the visible and near infrared ranges. The scattering is mainly caused by the randomly oriented heterogeneities of the refractive index that occur at the boundaries of the macromolecule structures, primarily, collagen fibers, with such heterogeneities being crucial in the formation of the skin optical properties [1].

In particular, these limitations are overcome by introducing biocompatible molecular agents into the tissue, which contribute to its optical clearing (OC) to some extent [1–9]. Quite a lot of summarized studies such as analytical reviews and monographs [10–14] have been devoted to experimental *in vivo*, *ex vivo* and *in vitro* implementations of the OC method on various types of biological tissues, which indicates the relevance of the problem. In [15] the researchers used optical coherence tomography (OCT) to visualize and quantitatively assess transdermal vaccine delivery. They demonstrated in real time how the OCT method may be applied to observe the impregnation of the vaccine microparticles into the skin. The paper [16] outlines the method of enhancing the visualization depth using OCT. The researchers used the method of optical clearing (OC) of the outer skin to reduce the light scattering and, thus, improve the quality and depth of the obtained images. This facilitated the process of studying in detail the tissues located deeper under the outer skin. Both studies demonstrate how OCT can be effectively applied in studying the skin processes, e.g., for studying the penetration of substances and improving the quality of visualization.

Many papers describe interesting applications of the method or prove its versatility and multimodality. For example, the use of this method in forensic applications for postmortem imaging of the perinatal dura mater and superior sagittal sinus using OCT method was outlined in paper [17]. The synergistic effect of an immersion agent (PEG-400), two chemical permeability enhancers of biological tissue (triazine and 1,2-propanediol) and mechanical massage on the effectiveness of rat skin OC was

evaluated *in vivo* by OCT methods in [18]. Urea is often used as one of the components in a mixture of various optical clearing agents (OCA) [11,19–21]. A mathematical model was proposed in [22] to solve the inverse problem of radiation transfer in biological tissues in order to determine the scattering and absorption coefficients for OC, taking into account the osmotic activity of OCA. Two approaches for noninvasive investigation of local diffusion of immersion OCA using OCT are described in [23]. The effect of model diabetes mellitus on OC of the skin of a laboratory mice was considered in paper [24] and a significant hindering of OCA diffusion in glycated tissues was shown. The mechanism of skin optical clearing was studied in [25] using glycerol and radiopaque drug Omnipaque® (iohexol) as OCA by imaging using auto-fluorescence with two-photon excitation and second harmonic generation (SHG-imaging). The paper [26] is devoted to elucidating mechanisms of OC of collagen tissue under normal conditions and under glycation using multiphoton tomography. The findings of studies of the dehydrating properties of OCA are presented in [27] and it is noted that dehydration is only one of the possible mechanisms leading to OC of biological tissues. Another mechanism for reducing the scattering cross-section of collagen fibers may be their reversible dissociation, which is also directly related to the molecular interaction of OCA and collagen [28]. Recently, a new approach has been proposed in study [29] to achieve optical transparency in biological tissues, which uses highly light-absorbing substances to change the refractive index of the aquatic environment. This leads to a significant reduction in light scattering. The study showed that food-grade water-soluble dyes such as tartrazine can make tissues transparent in the red and near-infrared regions of the spectrum. This method is based on increasing the real part of the refractive index of an aqueous biological medium (blood plasma, interstitial fluid, or cytoplasm) due to the phenomenon of anomalous dispersion and was proposed and studied in detail [30–34], where hemoglobin was used as an absorbing substance.

Studies in the field of the interaction of OCA with biological tissues open the way to understanding the physical and biophysical processes underlying OC at the molecular level [3,6,28,35–39]. This, in turn, will make it possible to find new effective OCA with specified properties that are optimal for a specific type of biological tissue.

The present work is a continuation of the authors' study of the molecular mechanisms at the post-diffusion stage of biological tissues OC [6,28,35–39] with an aqueous solution of urea as an example. In addition, starting with the study [38], the protocol of molecular modeling based on the semi-empirical PM6 method was replaced by the non-empirical Hartree-Fock (HF) method [40], since a preliminary study found that the semi-empirical method gives incorrect results for molecules with complex electronic structure, such as iohexol.

Experimental methods and results

Skin optical clearing *in vivo* was carried out using 50 %-aqueous solution of urea. The aqueous solution of urea was prepared by precise weighing: on a microanalytical balance (DA-225DC with calibration (0.001 g), Bel Engineering, Italy). The components of the solution were weighed and then transferred to a volumetric flask for dissolution and mixed thoroughly using a vortex mixer.

Refractive indices were measured using Abbe Atago DR-M2 1550 multi-wavelength refractometer (Atago, Japan) at 589 and 930 nm wavelengths at a temperature of 25.0 °C. The values of the refractive indices, molecular weights, and osmolality of the urea solutions are given in Table 1.

The OCT method was used to evaluate the optical clearing properties of the urea solution. In this work, a spectral-domain OCT GAN930V2-BU (Thorlabs, USA) with a central radiation wavelength of 930 ± 5 nm was used; the longitudinal resolution in air is $6.2\,\mu$m, and the transverse resolution is $9.6\,\mu$m; the size of the cross-scan area — 2 mm.

The study was conducted in accordance with the Declaration of Helsinki and was approved by the Ethics Committee of Saratov State Medical University named after V.I. Razumovsky (№ 11 dated August 7, 2022). The measurements were performed on the back of the forearm. Previously, the stratum corneum on this skin area was removed using medical tape, which was applied in 2×2 cm squares to the marked area pressed by the thumb with a force of 6N for 5 s. Three applications were made in total. Two-dimensional scans (B-scans) of the study area were recorded for 60 minutes with an interval of 3 minutes. Five volunteers between the ages of 25 and 57, of both sexes, participated in these measurements. A total of five measurements were made for the aqueous solution of urea.

The recorded OCT signal, according to the single scattering model [24,41–44], is described by the expression

$$R(z) \sim \exp(-\mu_t z), \tag{1}$$

where the attenuation coefficient

$$\mu_t = \mu_s + \mu_a, \tag{2}$$

z — is the scan depth.

Since the absorption coefficient μ_a of the skin is significantly less than the scattering coefficient μ_s in the range of 930−100 nm [1], the absorption coefficient μ_a may be neglected, so $R(z)$ can be approximated by the following expression [46]:

$$R(z) = A \exp(-\mu_s z) + B, \tag{3}$$

where A is the proportionality coefficient equal to $P_0 a(z)$, P_0 is the power of optical radiation incident on the skin surface, $a(z)$ is the local back reflectance, which characterizes the skin's ability to scatter light back and is determined by a local jump (fluctuation) in the refractive index, B is

Table 1. Physical properties of urea solution

Immersion agent	Chemical formula	Molecular weight,(g/mol)	Refraction index for $\lambda = 589$ nm	Refraction index for $\lambda = 930$ nm	Osmolality, (Osm/kg H_2O)
Urea 50 % aqueous solution	CH_4N_2O	60.06	1.407	1.3981	16.67*

Note. * Calculated value.

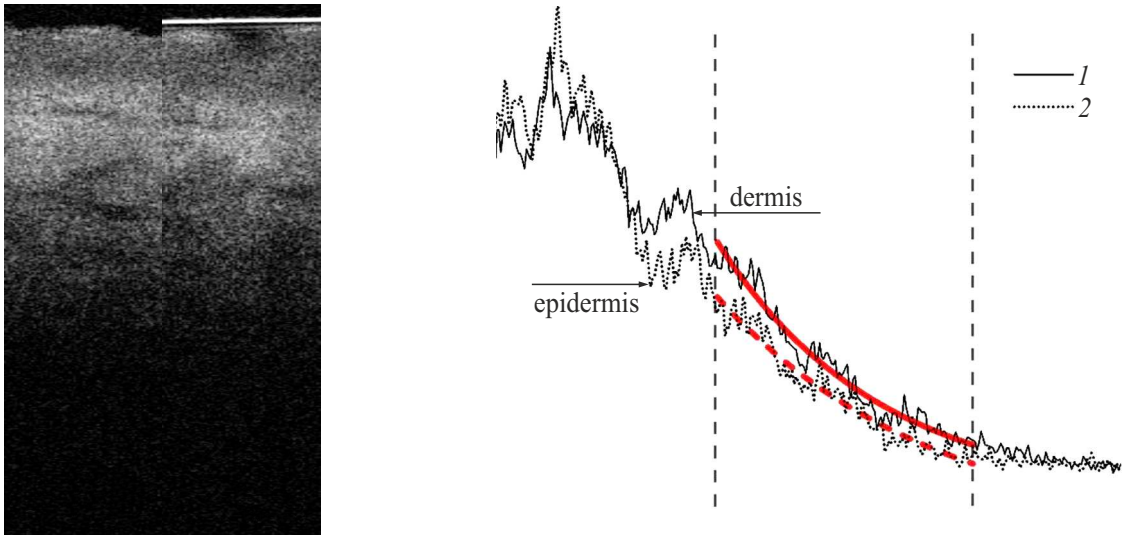

Figure 1. Measurements of the scattering coefficient μ_s in the dermis area after applying an urea solution based on OCT signal distribution analysis averaged over depth using a single scattering model: *a* — Image of a B-scan of the skin *in vivo*, according to a fragment of which the OCT signal was averaged immediately after applying and after 55 min exposure; *b* —depth distribution of the averaged OCT signals (thin curve) and the result of approximation according to the single scattering model (solid curves): *1* — right after applying the 50 %-aqueous solution of urea, *2* — after 55 min of exposure to urea, the vertical dashed straight lines denote the boundaries of the areas (from 350 to 700 μm) where μ_s was evaluated, the arrows indicate the layers of the skin: epidermis and dermis.

the background signal. The selection of coefficients in the above expression for approximating the experimental curve makes it possible to estimate the scattering coefficient of the object of study averaged over the selected segment of the depth of the longitudinal scan z. The single scattering model, often used in research, is an effective tool under certain conditions, but its application requires awareness of some limitations, associated, for instance, with the neglect of diffuse photon propagation and heterogeneity of such medium as the skin. When analyzing deeper layers of the skin or when very precise quantification is needed, more complex models allowing for multiple scattering may be needed.

Fig. 1 illustrates OCT images (B-scan) of the skin right after applying an aqueous solution of urea to it, and averaged A-scan of OCT signal of the dermal layer of human skin, as well as an approximating curve based on a single scattering model (3). OCT signals in the form of A-scans were averaged over the entire scan width of 2 mm along the skin surface. The scattering coefficient values were determined in the area of the averaged A-scan at depths from 350 to 700 μm.

From the Figure 1, *a*, it can be seen that over time, the image of the upper layers of the skin becomes darker, while the deeper layers become slightly lighter, which indicates that when affected by the urea solution upper layers of the skin demonstrate a lower light scattering, and light passes into the deeper layers, where it is reflected more intensely from the heterogeneities, which provides information about the deep-lying objects inside the tissue. Quantitatively, this is well reflected in Fig. 1, *b*.

Numerical values of the scattering coefficient obtained using an averaged A-scan in the dermis at depths from 350 to 700 μm were used to evaluate the optical clearing effectiveness (OCE) of the skin *in vivo*. The dependence of the scattering coefficients under the action of the urea solution on the observation time is shown in Fig. 2. It can be seen that for the urea solution, the value of the scattering coefficient μ_s over a long range of exposure times is well described by the linear regression model (the correlation coefficient R^2 is 97 %).

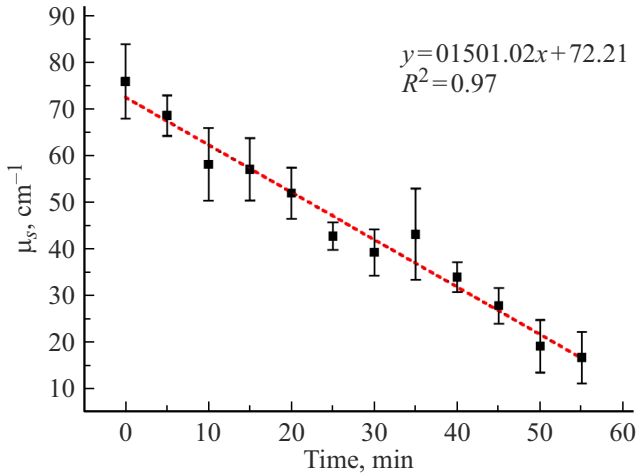

Figure 2. Time dependencies of the scattering coefficient μ_s in the dermal area (350–700 μm) of a human skin when exposed to 50 %-urea solution *in vivo*. The linear approximation is marked with a dashed line and expressed as an equation.

The values of the modulus of the average rate of decrease in the scattering coefficient were used for a numerical estimation of the OCE of human skin. This value is the slope coefficient determined from the regression line equations and numerically equal to 1.02 $cm^{-1}min^{-1}$.

Molecular modeling

The structures of the collagen mimetic peptide $((GPH)_3)_9$ [46] and its shortened version $((GPH)_3)_2$ (Fig. 3) selected by us for modeling represent the largest part of the regular domains of human collagen. Their spatial structure was constructed according to the Protein Data Bank (PDB). Hydrogen atoms were also added to the models, followed by optimization of their geometric structure by the method of molecular mechanics [47]. This model has some limitations because of the absence of some other kinds of triplets, e.g. Gly-Pro-Ala, Gly-Pro-Lys, that are also present in the native collagen. In addition, the model is limited in the length of the helix, which affects the stability and rigidity characteristic of native collagen. The structure shown in Fig. 3, *a* has a structurally molecular pocket about 10 x 15 angstrom in size which contains four functional groups: two hydroxyl groups (O_1H_1, O_2H_2) and two carbonyl groups (C_3O_3, C_4O_4) which form hydrogen bonds with OCA molecules. Three of them are located in one chain, and O_1H_1 group - on the other. The molecular modeling protocol consists of the following steps.

Construction and analysis of molecular structures of urea

The analysis of the considered urea molecule models was performed at the initial stage, using DFT/B3LYP/6-311+G(d,p) [48,49] method implemented in the Gaussian program [50]. The urea molecule may have two configurations: the first configuration with C_s symmetry (Fig. 3, *b*) and the second one with C_2 symmetry (Fig. 3, *c*). The configuration with C_2 symmetry has the lowest energy. The difference in energies makes 3.3 kJ/mol. To increase accuracy and provide better convergence in all calculations, stringent optimization criteria for geometry (opt=tight), self-consistent field (SCF=Tight) and integral grid (Int=UltraFine) were applied. The parameters of the urea molecular models calculated at this stage were further used in molecular dynamics and molecular docking. It should be noted that the modeling considers that part of the molecular process in which the immersion agent has already begun to interact directly with collagen.

Classical molecular dynamics

The intermolecular interaction of the urea molecules with collagen peptides was simulated at this stage using the GROMACS [51] classical molecular dynamics with the force field AMBER-03 [52]. The model scene consisted of a three-dimensional cell with periodic boundaries. The initial velocities of the atoms had a Maxwellian distribution and were set using a random number generator from the GROMACS package. During the simulation, the Berendsen thermostat and barostat [53] were used to ensure convergence of the thermodynamic parameters of the system to the following values:$T_0 = 307$ K, $P_0 = 1$ bar. The recorded trajectories of molecular motion were processed using GROMACS package and VMD (Visual Molecular Dynamics) program [54]. An example of the intermolecular interaction of the urea molecules with collagen peptide $((GPH)_3)_9$ is shown in Fig. 4, *a*.

Also, the change in protein volume is an informative parameter for establishing a correlation between the interaction of urea with the protein collagen and OCE [55]. Within the molecular modeling, the time dependence of changes in the volume of collagen peptides under the action of urea solution was investigated and two other commonly used OCA, such as glycerol and iohexol, were compared [39]. A fragment of collagen microfibril $5((GPH)_{12})_3$ was selected as the structure of the collagen mimetic peptide for modeling. For this peptide, the model scene consisted of a cell with side sizes 5 × 13 × 5 nm, in the center of which the collagen peptide was placed. The rest of the space was filled with a 50 %-urea aqueous solution (Fig. 4, *b, c*). The modeling time step was chosen to be 0.0001 ps, and the total modeling time was 1 ns. The system status was recorded every picosecond.

At the next stage of modeling, using molecular docking (AutoDockVina [56] program), the structures of hydrogen-bound complexes of the collagen peptide model and urea molecules were constructed. Ten most energetically stable configurations of intermolecular complexes were selected for the urea.

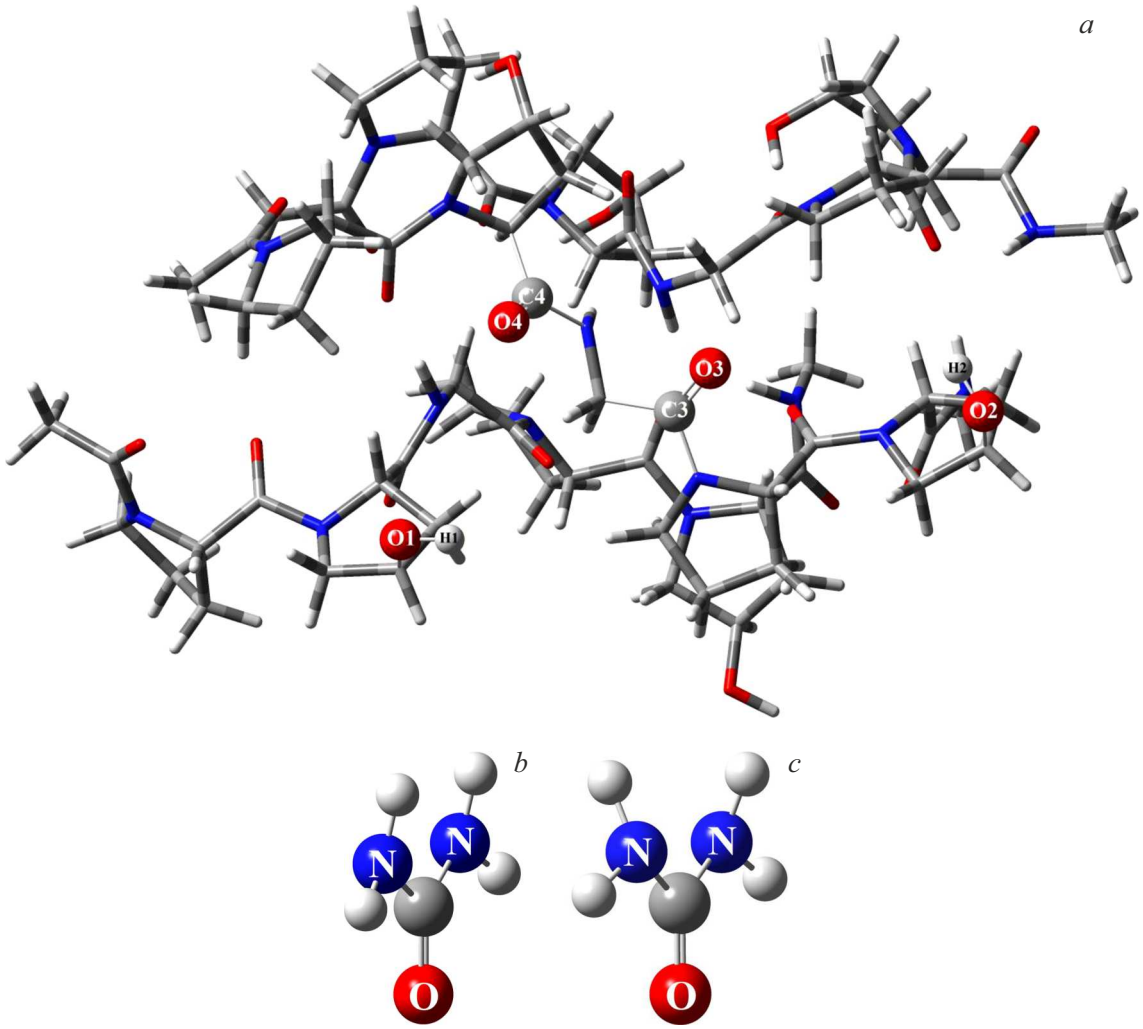

Figure 3. *a* — structure of the shortened collagen mimetic peptide $((GPH)_3)_2$, improved by the HF/STO-3G method (the atoms of the functional groups with which hydrogen bonds are formed are indicated). Two potential spatial structures of the urea molecule calculated by method B3LYP/6-311G+(d,p): *b* — symmetry type C_s, *c* — symmetry type C_2 (nitrogen and oxygen atoms are shown).

Methods of quantum chemistry

At this stage, structural optimization of all complexes of $((GPH)_3)_2$...-urea obtained by molecular docking was carried out using HF/STO3G method, followed by refinement of the electronic energy using a single SCF (self-consistent field) procedure using B3LYP/6-311G(d) method. The total electronic energy of the collagen peptide $((GPH)_3)_2$ and urea was calculated using a similar procedure. Further, the association energy was found by the formula

$$\Delta E = E_{\text{compl}} - E_{\text{GPH}} - 2E_{\text{M}}, \qquad (4)$$

where E_{compl} — total electronic energy of the complex $((GPH)_3)_2$-urea, E_{GPH} — total electronic energy of collagen peptide $((GPH)_3)_2$, E_{M} — total electronic energy of the urea molecule. Fig. 5 shows the inter-molecular complex $((GPH)_3)_2$...$(\text{urea})_2$ distinguished by maximal association energy. As can be seen from Fig. 5, urea molecules form a hydrogen bond with each other through amino groups, therefore, the energy of formation of this hydrogen bond was additionally calculated using the same method, which turned out to be 15.7 kJ/mol. This energy was subtracted from the energy of the association of urea with the collagen peptide.

For a more detailed study of the interaction of the urea molecule with collagen and with water molecules, six additional intermolecular complexes were analyzed, the structure of which is shown in Fig. 6. These studies were carried out using wB97XD [57] functional tailored for the analysis of non-valence interactions. In this case, the extended basis set 6-311+G(d,p) was used to eliminate the error associated with HF/STO-3G method and, accordingly, with the interpretation of the results.

As can be seen from Fig. 5, the urea molecule on the right forms hydrogen bonds with only one chain, so this part of the chain was cut out and GPH...urea complex was considered, the structure of which is shown in Fig. 6, *a*. To determine how urea competes with water

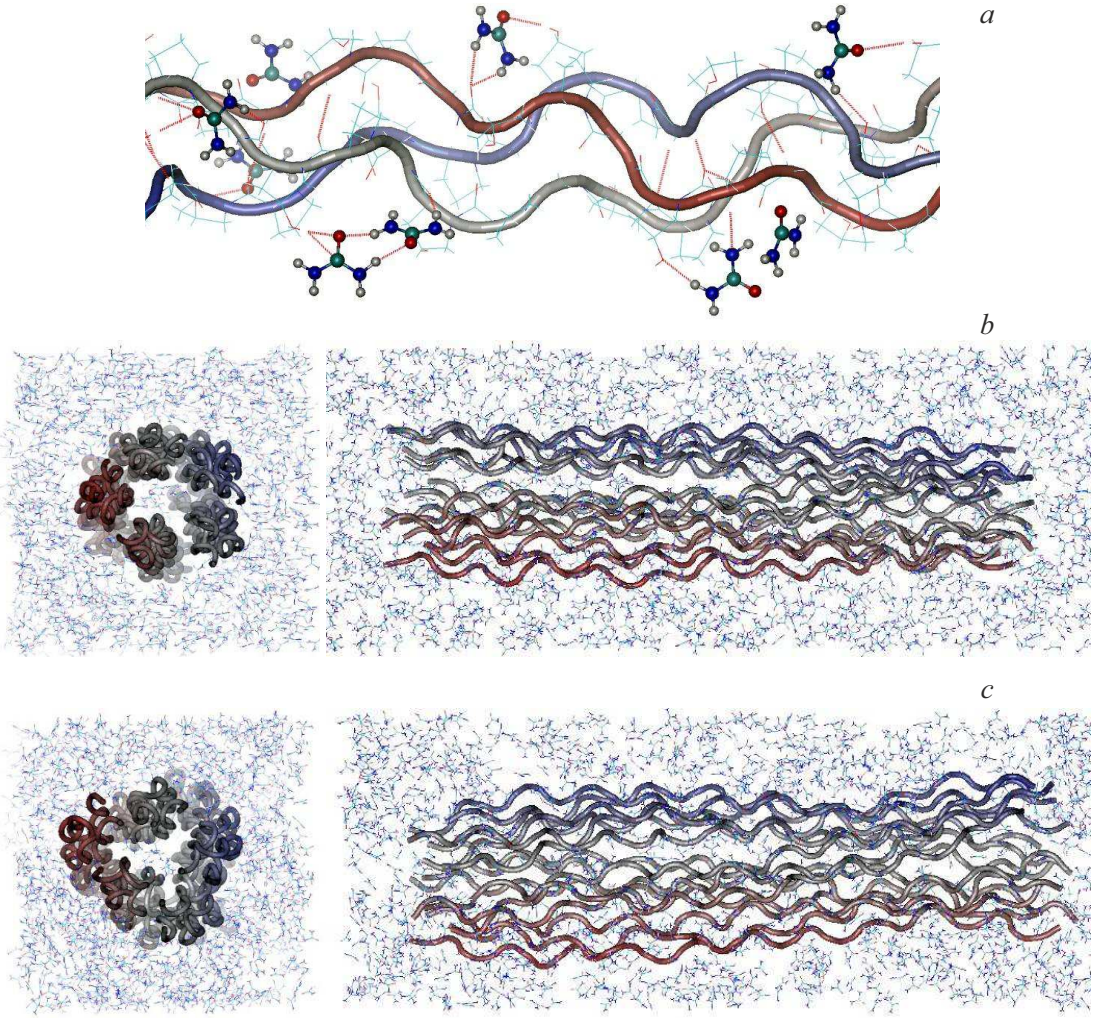

Figure 4. *a* — fragments of spatial structures of the hydrogen-bound collagen peptide complex $((GPH)_3)_9$ with urea molecules. Spatial distribution of urea molecules around the collagen peptide $5(GPH_{12})_3$, obtained in the framework of full-atomic molecular dynamics in two different projections: *b* — at the start of observation, *c* — after 1 ns.

molecules strongly bound to collagen, we examined the complex GPH. . .H_2O (Fig. 6, *b*). To analyze how strongly urea binds water molecules and affects the destruction of the water structure, accordingly, two different models of monohydrates were considered (Fig. 6, *c, d*) and the first urea hydrate shell was constructed (Fig. 6, *e*), and the water dimer was also considered (Fig. 6, *f*).

The intermolecular interaction energies were calculated taking into account the Basis Set Superposition Error ($BSSE$) [58]. We calculated the enthalpy of association of all six complexes for the temperatures $T = 0$ and $T = 310.15$ K using formula

$$\Delta H_T^0 = \Delta E + \Delta ZPE + BSSE + \Delta H_{\text{term}}, \qquad (5)$$

where ΔE is the difference of total electronic energies of the complex and monomers, ΔZPE is the difference of zero vibrational energies, $BSSE$ is the superposition error, ΔH_{term} is the thermodynamic correction found by the formulae [55]. The equilibrium constant K_T was found by the formula

$$K_T = \exp\left(-\frac{\Delta G^0}{RT}\right), \qquad (6)$$

where ΔG^0 is the Gibbs free energy change, R is the gas constant, T is the temperature. The numerical values of these parameters are given in Table 2.

Discussion of the results

Experimental data (Fig. 7) show that a 50 %-solution of urea is a fairly effective OCA for human skin and has OCE comparable to solutions of ribose and sucrose. The obtained value is in good agreement with the linear regression relationship between OCE and the energy of intermolecular interaction.

Molecular modeling performed using all-atom molecular dynamics shows that two urea molecules can fit into the

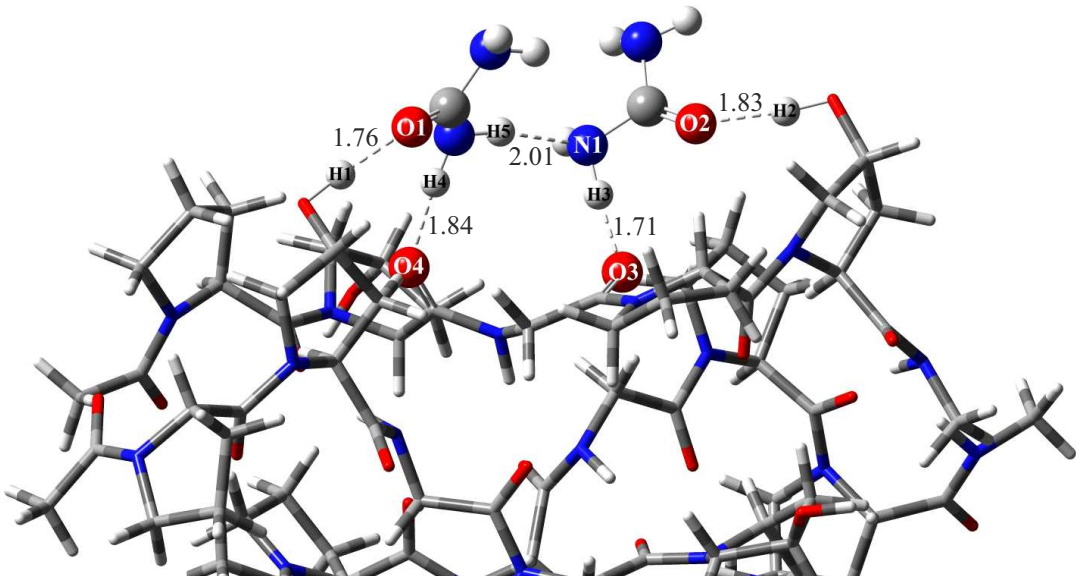

Figure 5. Fragment of molecular model of collagen peptide complex $((GPH)_3)_2$ with two molecules of urea improved by HF/STO-3G method. The dashed lines in the figure show intermolecular hydrogen bonds. The atoms involved in the formation of hydrogen bonds and the lengths of hydrogen bonds (in angstroms) are indicated).

Table 2. Thermodynamic parameters of intermolecular complexes (in units of kJ/mol) and equilibrium constants calculated using *BSSE* method wB97XD/6-311+G(d,p)

Intermolecular complex	*BSSE*	ΔZPE	ΔE	ΔH_0^0	$\Delta H_{310.15}^0$	$T\Delta S$	$K_{310.15}$
GPH... H_2O	7.5	9.7	−51.7	−34.5	−37.0	−42.3	1.3E−01
GPH... urea	4.4	3.3	−51.2	−43.5	−41.3	−42,3	6.8E−01
Dimer H_2O	3.4	10.0	−26.4	−13.0 13.22 ± 0.12[1] [59]	−15.4 15.454 ± 0.074[2] [60]	−28.0	7.6E−03
Urea... H_2O[3]	2.7	9.7	−45.6	−33.2	−35.6	−37.3	5.2E−01
Urea... H_2O[4]	3.5	6.6	−31.8	−21.6	−21.6	−32.0	1.8E−02
Urea... $(H_2O)_7$	35.0[5]	72.9	−316.4	−208.6 −29.8[6]	–	–	–

Note. [1] Original experimental value $1105 \pm 10\,cm^{-1}$ is transformed into kJ/mol. [2] The value is obtained using active thermochemical tables. [3] Structure of urea monohydrate (Fig. 7, *c*). [4] Structure of urea monohydrate(Fig. 7, *d*). [5] Parameter *BSSE* was calculated using the partial *BSSE* method, when the values calculated for each water molecule are added together. [6] The value expressed as one water molecule.

molecular pocket of a collagen peptide at a time and form dimeric structures (Fig. 4, *a*). Urea molecules interact with collagen by forming four hydrogen bonds. The first urea molecule (left in Fig. 5) forms one hydrogen bond with the proton of the hydroxyl group of hydroxyproline of one chain, and the second with the carbonyl group of proline of the other chain. The second urea molecule forms bonds with the proton of the hydroxyl group of hydroxyproline and with the carbonyl group of glycine of the same chain. In addition, urea molecules form a hydrogen bond between themselves through amino groups.

From the analysis of the data given in Table 2, it can be seen that collagen interacts more intensely with urea than with water molecules. The enthalpy of association of collagen with urea (−41.3 kJ/mol) is more negative than with water (−37.0 kJ/mol), which indicates a more energetically beneficial binding to urea. Also, the equilibrium constant for the urea complex is (0.68) higher than for the water complex (0.13), which indicates a greater stability of the urea complex. Thus, urea greatly competes with water molecules, substituting it in the vicinity of collagen. This can lead to the displacement of water molecules from the hydrate shell of collagen, disrupting its structure, which is consistent with the well-known denaturing effect of urea. The enthalpy of association of the urea monohydrates −35.6 and −21.6 kJ/mol has a modulus less than GPH...urea complex. The complete first hydrate shell of the urea molecule, according to the simulation, has seven water molecules. The addition of the water molecule to any structural position leads to the formation of a bridge of a water molecule that is no longer directly bound to the urea molecule and belongs to the second hydrate shell. The

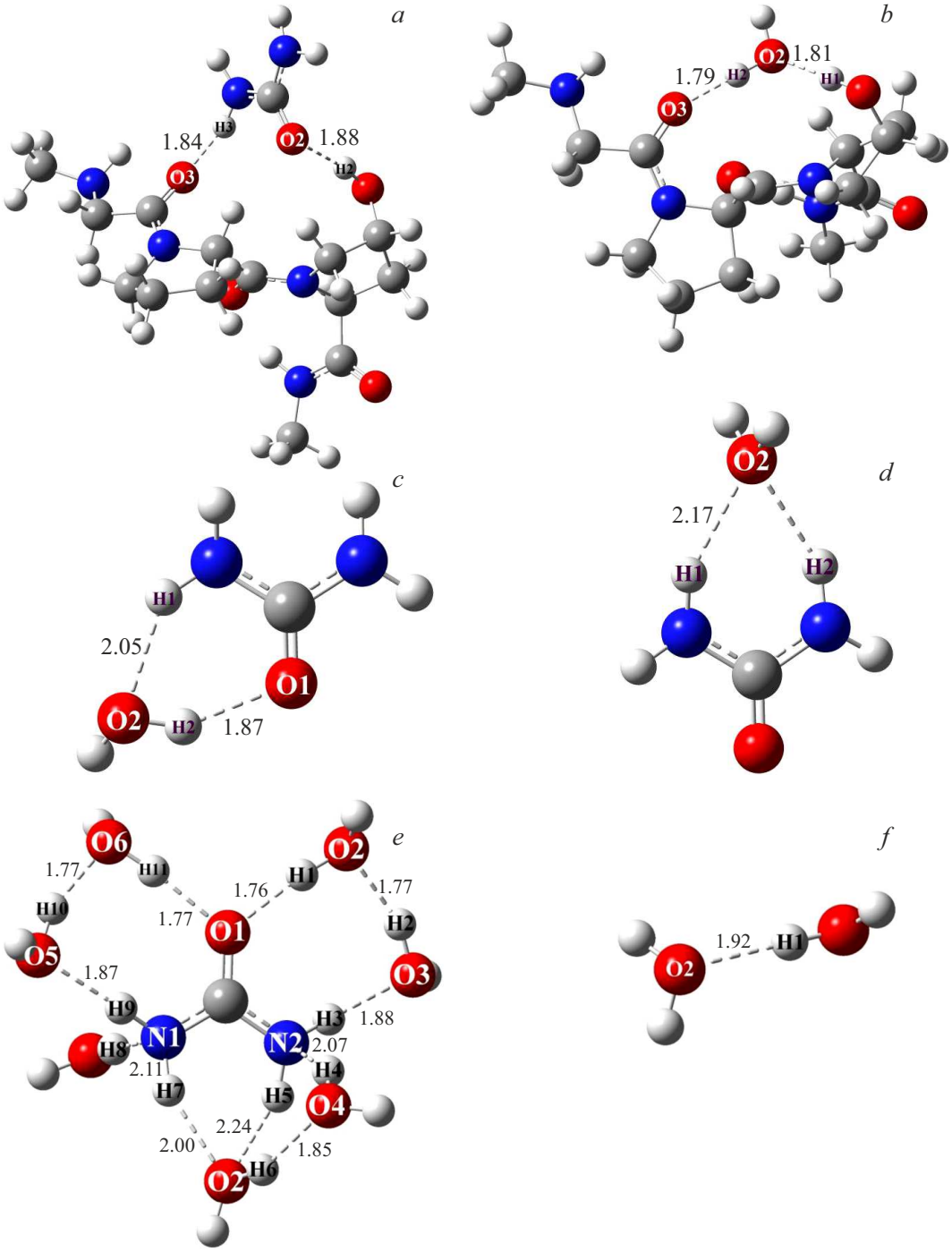

Figure 6. Molecular models of complexes wB97XD/6-311G+(d,p): *a* — urea with a chain of three amino acid residues proline, hydroxyproline and glycine (GPH); *b* — GPH. . .H_2O; *c, d* — urea. . .H_2O; *e* — the first hydrate shell of the urea molecule; *f* — water dimer. The dashed lines show hydrogen bonds. The lengths of the hydrogen bonds (in angstroms) and the atoms involved in the formation of the hydrogen bond are indicated.

enthalpy per water molecule is −29.8 kJ/mol, which is also less than that for GPH. . .urea complex. This means that when interacting with collagen, urea may partially lose its hydration shell. The bond between free water molecules is much weaker than the interactions considered, so urea easily destroys the water structure. That is, the urea molecule, having proton donors and acceptors during the formation of hydrogen bonds, is able to integrate into the water network and destroy it. This leads to an increase in the mobility of water molecules and a decrease in the overall order of the water structure. Water becomes less structured which impact its properties. This allows the urea molecules

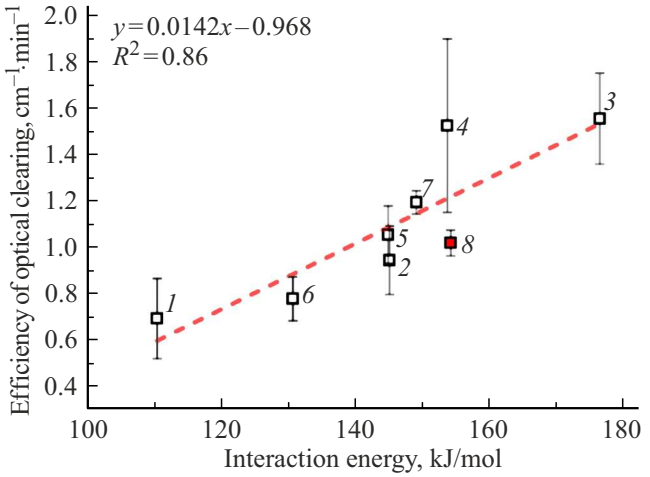

Figure 7. Human skin OCE *in vivo* versus energy of the intermolecular interaction of the collagen peptide fragment $((GPH)_3)_2$ and various OCAs [38,39]: glycerol (*1*), ribose (*2*), dextrose (*3*), fructose (*4*), sucrose (*5*), glucosamine (*6*), iohexol (*7*), urea (*8*). The linear approximation is marked with a dashed line and expressed as an equation.

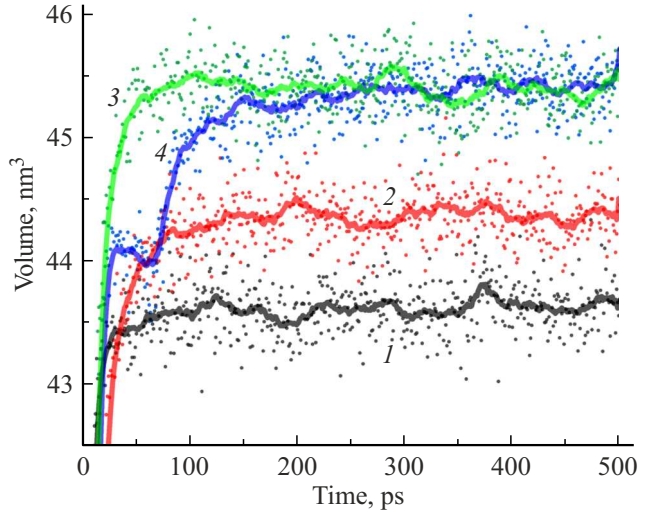

Figure 8. Volume of collagen peptide versus time of exposure to OCA: without OCA (pure water) (*1*), 50 %-aqueous solution of urea (*2*), 60 %-aqueous solutions of glycerol (*3*) and iohexol (*4*) [38].

to approach the surface of the collagen. Further, urea competes with water for the formation of hydrogen bonds with collagen. Since urea can form stronger hydrogen bonds with some parts of collagen, it displaces water molecules from the hydrate shell. This initially leads to an increase in the volume of collagen due to reversible dissociation (the distance between the microfibrils becomes larger). This conclusion is confirmed by the results of modeling shown in Fig. 8, *a*. Further, at significant concentrations (from 25, % and higher) and more significant interaction times (on the order of hundreds of nanoseconds), collagen denaturation (unfolding of the triple helix of microfibrils) occurs. It should be noted that when a 50% aqueous solution of urea is applied to the skin, units of percent penetrate into the dermis area. Therefore, no collagen denaturation occurs. With this in mind, the simulation times for plotting the graph in Fig. 8 were taken small. The data presented in Fig. 8 are qualitative in nature and show how different immersion agents affect the volume of collagen.

From Fig. 8 it can be seen that as a result of the destruction of the aqueous structure, an increase in the volume of collagen occurs, which is also illustrated in Fig. 4, *b, c*. That is, the process of reversible dissociation of collagen microfibrils occurs. These structural changes affect the reduction of the refractive index of collagen by lowering the collagen concentration; the difference with the refractive index of the intercellular fluid mixed with the immersion agent becomes less, which accordingly is benign for the skin treatment process.

Conclusion

Based on experimental *in vivo* data, the OCE of human skin was determined with the use of 50 % aqueous urea solution. The complex molecular modeling of the interaction of urea with a model collagen peptide showed that the obtained parameters for urea are in good consistency with the linear regression between the energy of intermolecular interaction and the OCE of human skin. This allows the regression equation to be used for predictive purposes. Urea forms more stable complexes with collagen than water, and can effectively displace water from the hydrate shell of collagen, disrupting the structure of hydrogen bonds and leading to reversible dissociation of collagen structures and, consequently, to a lower refractive index. Thus, the faster the diffusion process takes place and the greater the energy of the immersion agent's association with collagen, the higher the OCE. The urea molecule has a stable hydrate shell, but its interaction with collagen (based on the simulation results) turns out to be thermodynamically more beneficial than maintaining a complete hydrate shell. With the help of the conducted research, the value of the parameters of the linear regression equation has been clarified.

The findings of the study serve the basis for the development of new non-invasive techniques for improving visualization of dermal and hypodermal structures in clinical practice. In particular, the technique can be useful: in dermatology — for more accurate diagnosis of skin neoplasms and inflammatory processes using OCT; in laser therapy and cosmetology — to increase the depth of laser radiation penetration while minimizing scattering; when monitoring microcirculation and the state of the collagen matrix in the assessment of wound healing, fibrosis and age-related skin changes.

The use of urea as a component of the clearing agent is attractive because it is already used in dermatological

preparations (including medical creams and ointments) and has a known safety profile for external use.

Despite the demonstrated effectiveness, the use of highly concentrated urea solutions has a number of limitations. These may include potential skin irritation: with prolonged exposure or hypersensitivity, irritation or hyperemia may develop, especially if the integrity of the skin is compromised. The effect of OC is temporary and depends on the degree of tissue hydration, agent concentration, and exposure time. Individual skin features: thickness, collagen density, and hydration vary from patient to patient, which requires a personalized approach to choosing the right concentration and exposure time.

Funding

The work has been funded by the grant (№ 23-14-00287) from the Russian Science Foundation.

Conflict of interest

The authors declare that they have no conflict of interest.

References

[1] V.V. Tuchin. *Tissue Optics: Light Scattering Methods and Instruments for Medical Diagnostics*, 3rd ed. (SPIE Press, Bellingham, WA, 2015). DOI: 10.1117/3.1003040

[2] H. Jonasson, I. Fredriksson, S. Bergstrand, C.J. Östgren, M. Larsson, T. Strömberg. J. Biomed. Opt., **23** (12), 121608 (2018). DOI: 10.1117/1.JBO.23.12.121608

[3] *Handbook of Tissue Optical Clearing: New Prospects in Optical Imaging*, ed. by V.V. Tuchin, D. Zhu, E.A. Genina (Taylor & Francis Group LLC, CRC Press, Boca Raton, FL, 2022). DOI: 10.1201/9781003025252

[4] J.M. Hirshburg. *Chemical agent induced reduction of skin light scattering: doctoral dissertation* (Texas A & M University, 2009).

[5] D. Zhu, K.V. Larin, Q. Luo, V.V. Tuchin. Laser Photonics Rev., **7** (5), 732 (2013). DOI: 10.1002/lpor.201200056

[6] A.N. Bashkatov, K.V. Berezin, K.N. Dvoretskiy, M.L. Chernavina, E.A. Genina, V.D. Genin, V.I. Kochubey, E.N. Lazareva, A.B. Pravdin, M.E. Shvachkina, P.A. Timoshina, D.K. Tuchina, D.D. Yakovlev, D.A. Yakovlev, I.Yu. Yanina, O.S. Zhernovaya, V.V. Tuchin. J. Biomed. Opt., **23** (9), 091416 (2018). DOI: 10.1117/1.JBO.23.9.091416

[7] M. Kirillin, I. Meglinski, V. Kuzmin, E. Sergeeva, R. Myllylä. Opt. Express, **18** (21), 21714 (2010). DOI: 10.1364/OE.18.021714

[8] I. Meglinski, M. Kirillin, V. Kuzmin, R. Myllylä. Opt. Lett., **33** (14), 1581 (2008). DOI: 10.1364/OL.33.001581

[9] I.V. Meglinskii, V.L. Kuz'min, A.V. Priezzhev. Quant. Electron., **36** (11), 989 (2006). DOI: 10.1070/QE2006v036n11ABEH013458

[10] L. Oliveira, V.V. Tuchin. *The Optical Clearing Method: A New Tool for Clinical Practice and Biomedical Engineering* (Basel: Springer Nature Switzerland AG, 2019). DOI: 10.1007/978-3-030-33055-2

[11] I. Costantini, R. Cicchi, L. Silvestri, F. Vanzi, F.S. Pavone. Biomed. Opt. Express, **10** (10), 5251 (2019). DOI: 10.1364/boe.10.005251

[12] P. Matryba, L. Kaczmarek, J. Gołąb. Laser Photonics Rev., **13** (8), 1800292 (2019). DOI: 10.1002/lpor.201800292

[13] T. Yu, J. Zhu, D. Li, D. Zhu. iScience, **24** (3), 102178 (2021). DOI: 10.1016/j.isci.2021.102178

[14] I.S. Martins, H.F. Silva, E.N. Lazareva, N.V. Chernomyrdin, K.I. Zaytsev, L.M. Oliveira, V.V. Tuchin. Biomed. Opt. Express, **14** (1), 249 (2023). DOI: 10.1364/BOE.479320

[15] T. Kamali, A. Doronin, T. Rattanapak, S. Hook, I. Meglinski. Laser Phys. Lett., **9** (8), 607 (2012). DOI: 10.7452/lapl.201210046

[16] S.G. Proskurin, I.V. Meglinski. Laser Phys. Lett., **4** (11), 824 (2007). DOI: 10.1002/lapl.200710056

[17] E.C. Cheshire, R.D.G. Malcomson, S. Joseph, A. Adnan, D. Adlam, G.N. Rutty. Int. J. Legal Med., **131**, 1377 (2017). DOI: 10.1007/s00414-017-1570-1

[18] T. Yu, J. Zhu, Y. Li, Y. Ma, J. Wang, X. Cheng, S. Jin, Q. Sun, X. Li, H. Gong, Q. Luo, F. Xu, S. Zhao, D. Zhu. Sci. Rep., **8** (1), 1964 (2018). DOI: 10.1038/s41598-018-20306-3

[19] L. Chen, G. Li, Y. Li, Y. Li, H. Zhu, L. Tang, P. French, J. McGinty, Sh. Ruan. Sci. Rep., **7**, 12218 (2017). DOI: 10.1038/s41598-017-12484-3

[20] H. Soleimanzad, M. Juchaux, H. Gurden, D. Crepin, F. Pain. Proc. SPIE, **11226**, 1122614 (2020). DOI: 10.1117/12.2544298

[21] M.S. Lai, W.M. Chick, M.H. Law, R.Ch. Chang. Sci. Rep., preprint (2025). DOI: 10.21203/rs.3.rs-6517663/v1

[22] X. Wen, S.L. Jacques, V.V. Tuchin, D. Zhu. J. Biomed. Opt., **17** (6), 066022 (2012). DOI: 10.1117/1.JBO.17.6.066022

[23] A.N. Bashkatov, E.A. Genina, V.V. Tuchin. *Handbook of Optical Sensing of Glucose in Biological Fluids and Tissues*, ed. by V.V. Tuchin (Taylor & Francis Group LLC, CRC Press, 2009), ch. 21. DOI: 10.1201/9781584889755

[24] K.V. Larin, V.V. Tuchin. Quant. Electron., **38** (6), 551 (2008). DOI: 10.1070/QE2008v038n06ABEH013850.

[25] D.K. Tuchina, R. Shi, A.N. Bashkatov, E.A. Genina, D. Zhu, Q. Luo, V.V. Tuchin. J. Biophotonics, **8** (4), 332 (2015). DOI: 10.1002/jbio.201400138

[26] V. Hovhannisyan, P.-S. Hu, S.-J. Chen, C.-S. Kim, C.-Y. Dong. J. Biomed. Opt., **18** (4), 046004 (2013). DOI: 10.1117/1.JBO.18.4.046004

[27] A.Yu. Sdobnov, M.E. Darvin, E.A. Genina, A.N. Bashkatov, J. Lademann, V.V. Tuchin. Spectrochimica Acta A, **197**, 216 (2018). DOI: 10.1016/j.saa.2018.01.085

[28] A.T. Yeh, B. Choi, J.S. Nelson, B.J. Tromberg. J. Inv. Derm., **121** (6), 1332 (2003). DOI: 10.1046/j.1523-1747.2003.12634.x

[29] Z. Ou, Yi-Sh. Duh, N.J. Rommelfanger, C.H.C. Keck, Sh. Jiang, K. Brinson Jr., S. Zhao, E.L. Schmidt, X. Wu, F. Yang, B. Cai, H. Cui, W. Qi, Sh. Wu, A. Tantry, R. Roth, J. Ding, X. Chen, J.A. Kaltschmidt, M.L. Brongersma, G. Hong. Science, **385** (6713), eadm6869 (2024). DOI: 10.1126/science.adm686

[30] V.V. Tuchin, D.M. Zhestkov, A.N. Bashkatov, E.A. Genina. Optics Express, **12** (13), 2966 (2004). DOI: 10.1364/OPEX.12.002966

[31] V.V. Tuchin. *Optical Clearing of Tissues and Blood* (SPIE Press, Bellingham, WA, 2005). DOI: 10.1117/3.637760

[32] O. Sydoruk, O. Zhernovaya, V. Tuchin, A. Douplik. J. Biomed. Opt., **17** (11), 115002-1-6 (2012). DOI: 10.1117/1.JBO.17.11.115002
[33] O. Zhernovaya, V.V. Tuchin, M.J. Leahy. J. Biomed. Opt., **18** (2), 026014-1-8 (2013). DOI: 10.1117/1.JBO.18.2.026014
[34] O.S. Zhernovaya, E.A. Genina, V.V. Tuchin, A.N. Bashkatov. *Handbook of Tissue Optical Clearing: New Prospects in Optical Imaging*, ed. by V.V. Tuchin, D. Zhu, E.A. Genina (Taylor & Francis Group LLC, CRC Press, Boca Raton, FL, 2022). P. 383–392. DOI: 10.1201/9781003025252
[35] T. Yu, X. Wen, V.V. Tuchin, Q. Luo, D. Zhu. J. Biomed. Opt., **16** (9), 095002 (2011). DOI: 10.1117/1.3621515
[36] X. Wen, Z. Mao, Z. Han, V.V. Tuchin, D. Zhu. J. Biophotonics, **3** (1−2), 44 (2010). DOI: 10.1002/jbio.200910080
[37] A.Yu. Sdobnov, M.E. Darvin, J. Schleusener, J. Lademann, V.V. Tuchin. J. Biophotonics, **12** (5), e201800283 (2019). DOI: 10.1002/jbio.201800283
[38] K.V. Berezin, E.V. Grabarchuk, A.M. Lichter, K.N. Dvoretski, V.V. Tuchin. J. Biophotonics, **17** (2), e202300354 (2024). DOI: 10.1002/jbio.202300354
[39] K.V. Berezin, E.V. Grabarchuk, A.M. Lichter, K.N. Dvoretski, Yu.I. Surkov, V.V. Tuchin. Techn. Phys., **69** (3), 485 (2024). DOI: 10.21883/0000000000.
[40] C.C.J. Roothaan. Rev. Mod. Phys., **23** (2), 69 (1951). DOI: 10.1103/RevModPhys.23.69
[41] D.J. Faber, F.J. van der Meer, M.C.G. Aalders, T.G. van Leeuwen. Opt. Express, **12** (19), 4353 (2004). DOI: 10.1364/OPEX.12.004353
[42] P. Lee, W. Gao, X. Zhang. Appl. Opt., **49** (18), 3538 (2010). DOI: 10.1364/AO.49.003538
[43] E.A. Genina, A.N. Bashkatov, E.A. Kolesnikova, M.V. Basko, G.S. Terentyuk, V.V. Tuchin. J. Biomed. Opt., **19** (2), 021109 (2014). DOI: 10.1117/1.JBO.19.2.021109
[44] R.K. Wang, V.V. Tuchin. *Handbook of Coherent-Domain Optical Methods. Biomedical Diagnostics, Environmental Monitoring, and Material Science*. V. 2, 2nd ed., ed. by V.V. Tuchin (Berlin, Heidelberg, N.Y.: Springer-Verlag, 2013). P. 665. DOI: 10.1007/978-1-4614-5176-1
[45] E.A. Genina, N.S. Ksenofontova, A.N. Bashkatov, G.S. Terentyuk, V.V. Tuchin. Quant. Electron., **47** (6), 561 (2017). DOI: 10.1070/QEL16378.
[46] K. Okuyama, K. Miyama, K. Mizuno, H.P. Bachinger. Biopolymers, **97** (8), 607 (2012). DOI: 10.1002/bip.22048
[47] W.D. Cornell, P. Cieplak, C.I. Bayly, I.R. Gould, K.M.Jr. Merz, D.M. Ferguson, D.C. Spellmeyer, T. Fox, J.W. Caldwell, P.A. Kollman. J. Am. Chem. Soc., **117** (19), 5179 (1995). DOI: 10.1021/ja00124a002
[48] A.D. Becke. J. Chem. Phys., **98** (7), 5648 (1993). DOI: 10.1063/1.464913
[49] C. Lee, W. Yang, R.G. Parr. Phys. Rev. B, **37** (2), 785 (1988). DOI: 10.1103/PhysRevB.37.785
[50] M.J. Frisch, G.W. Trucks, H.B. Schlegel et al. *Gaussian09, Revision A.02* (Pittsburgh PA: Gaussian, Inc. 2009).
[51] D. Van der Spoel, E. Lindahl, B. Hess, G. Groenhof, E.A. Mark, H.J.C. Berendsen. J. Comput. Chem., **26** (16), 1701 (2005). DOI: 10.1002/jcc.20291
[52] Y. Duan, C. Wu, S. Chowdhury, M.C. Lee, G. Xiong, W. Zhang, R. Yang, P. Cieplak, R. Luo, T. Lee, J. Caldwell, J. Wang, P. Kollman. J. Comp. Chem., **24** (16), 1999 (2003). DOI: 10.1002/jcc.10349
[53] H.J.C. Berendsen, J.P.M. Postma, W.F. van Gunsteren, A. DiNola, J.R. Haak. J. Chem. Phys., **81** (8), 3884 (1984). DOI: 10.1063/1.448118
[54] W. Humphrey, A. Dalke, K. Schulten. J. Mol. Graph., **14** (1), 33 (1996). DOI: 10.1016/0263-7855(96)00018-5
[55] K.V. Berezin, K.N. Dvoretski, M.L. Chernavina, A.M. Likhter, V.V. Smirnov, I.T. Shagautdinova, E.M. Antonova, E.Yu. Stepanovich, E.A. Dzhalmuhambetova, V.V. Tuchin. J. Mol. Modeling., **24** (2), 45 (2018). DOI: 10.1007/s00894-018-3584-0
[56] O. Trott, A.J. Olson. J. Comput. Chem., **31** (2), 455 (2010). DOI: 10.1002/jcc.21334
[57] J.-D. Chai, M. Head-Gordon. J. Chem. Phys., **128** (8), 084106 (2008). DOI: 10.1063/1.2834918
[58] S. Simon, M. Duran, J.J. Dannenberg. J. Chem. Phys., **105** (24), 11024–11031 (1996). DOI: 10.1063/1.472902
[59] B.E. Rocher-Casterline, L.C. Ch'ng, A.K. Mollner, H. Reisler. J. Chem. Phys., **134** (21), 211101 (2011). DOI: 10.1063/1.3598339
[60] B. Ruscic. J. Phys. Chem. A, **117** (46), 11940 (2013). DOI: 10.1021/jp403197t

Translated by J.Savelyeva